PHYSICAL REVIEW B VOLUME 55, NUMBER 13 1 APRIL 1997-I

High-field paramagnetic effect in large crystals of $YBa_2Cu_3O_{7-\delta}$

A. I. Rykov and S. Tajima
Superconductivity Research Laboratory, Interational Superconductivity Technology Center, 10-13, Shinonome 1-Chome, Koto-ku, Tokyo, 135 Japan

F. V. Kusmartsev*
Nordisk Institute for Theoretisk Fysik, Blegdamsvej 17, DK 2100 Copenhagen ∅, Denmark and Landau Institute for Theoretical Physics, Moscow 117940, Russia

(Received 15 July 1996; revised manuscript received 17 October 1996)

We observed the appearance of a paramagnetic moment in $YBa_2Cu_3O_{7-\delta}$ single crystals after cooling in a strong field (3–7 T). It is found that the effect depends on the cooling rate and sample size, indicating that the paramagnetic moment can be induced by compression of the magnetic flux in the course of rapid cooling. After rapid cooling, the temperature dependence of the magnetization during the field-cooled warming process exhibits a very articulated negative dip between irreversibility temperature $T_{\rm irr}$ and T_c. The diamagnetic dip may result from escaping the compressed flux. Comparing the dip widths for a number of crystals with different irreversibility lines $H_{\rm irr}(T)$ we found that a remarkable ''fishtail'' effect appears in the temperature region below the dip. This suggests that the field-induced pinning observed by the fishtail effect is linked with the paramagnetic effect that appears after rapid cooling in the high field. [S0163-1829(97)07713-8]

I. INTRODUCTION

It is widely recognized that both cuprate and conventional low-T_c superconductors may exhibit a paramagnetic moment after cooling in a small field.[1–3] This effect was observed initially in granular ceramic samples of high-T_c superconductors.[4–6] Since the effect was observed in the Meissner range of a magnetic field, it was called a ''paramagnetic Meissner effect'' (PME) or ''Wohlleben effect.''[7] Two alternative concepts explaining this effect were proposed.[1,8] First, the effect was understood in the physical picture of a polarizable glassy state composed of circular currents. The spontaneous generation of the orbital currents was attributed to the existence in granular superconductors of Josephson π links.[9] This picture explained the observed field dependence of the effect: The lower the external field, the higher the paramagnetic susceptibility.[8] Owing to thermally activated flipping of the orbital moments the spontaneous paramagnetic magnetization increases with the age of the system.[10,11] The required π-phase shift for the Josephson junction in this model was assigned to the impurity levels identified with some oxygen defects[9] or, more intrinsically, to an unconventional order parameter.[7] The latter origin of the phase shift, however, is unexpected for the recently reported low-field PME (LFPME) observed after field cooling in Nb samples.[2,3]

Another explanation of the low-field paramagnetic effect was proposed recently by Koshelev and Larkin.[1] They calculated the magnetic moment for both complete and incomplete Bean critical states with a flux compressed in a thin strip and in a thin disk. According to Ref. 1, the Bean state with a compressed flux can be stabilized, for example, as a result of inhomogeneous cooling. The incomplete Bean state may appear in the sample in the case of vanishing critical current for some of the sample regions. Although flux trapping alone cannot explain the Wohlleben effect,[7] the magnetization could become paramagnetic if a compression of the trapped flux was allowed.[1] This scenario involves a formation of an essentially flux-free layer near the equatorial surface of the sample. The flux is expelled from the surface layer toward the inside region. The authors[1] claim that the degree of the compression of trapped flux would be larger for smaller fields; therefore, their model also adequately describes the observed dependence of the PME on the applied field.

In this work, we report on the observation of the paramagnetic moment in large and thick high-quality $YBa_2Cu_3O_{7-\delta}$ single crystals. The paramagnetic moment appears if we cool the sample from above T_c in a fixed strong magnetic field (3–7 T). Also, in very small fields (below 1 Oe), we observed some qualitative marks of paramagnetic behavior in our samples; however, we do not focus on the studies of these low-field effects. With increasing the external field above a few Oe, all the samples showed the conventional Meissner effect; at these fields the absolute value of the field-cooled (FC) magnetization increased with increasing field ($\chi = \text{const}$). The key discovery of our work is that further increasing the applied field quite far above H_{c1} (up to $\mu_0 H$ approximately 3–7 T) also results in the appearance of the paramagnetic moment in the sample, $\chi > 0$. We call this phenomenon a ''high-field para-magnetic effect'' (HFPME).

Remarkably, the shape of the susceptibility curves is quite similar to the one reported for small fields.[4–6] In detail, the field-cooled magnetization becomes negative in close vicinity of T_c, showing a pronounced dip below T_c; however, upon lowering the temperature the FC magnetization gradually increases up to a positive value and retains a nearly constant value in a broad temperature range. We observed that the temperature region of the negative dip in magnetization curves closely corresponds to the gap between the critical temperature $T_c(H)$ and irreversibility line $T_{\rm irr}(H)$. The

similarity in the temperature dependence of magnetization suggests that there may exist a close analogy between two phenomena.

II. EXPERIMENTAL DETAILS

Single crystals of $YBa_2Cu_3O_{7-\delta}$ were prepared by a pulling technique and untwinned as described previously.[12] Three large as-grown crystals were cut and detwinned. Seven pieces were selected after the detwinning and annealing procedure as described in Ref. 12. The crystals were characterized by x-ray diffraction and Raman spectroscopy and showed quite the usual structure and phonon parameters. The appearance of the HFPME was qualitatively detected on all seven pieces. A set of detailed data was obtained on the two samples. Sample 1 had an optimal T_c of 92.3 K with a very narrow transition width of 0.04 K. The dimensions of this crystal were $3.8\times1.9\times1.7$ mm^3 ($a\times b\times c$). The final annealing of this sample was done at 490 °C to get the optimal value of T_c. Another crystal (sample 2) was overdoped at 400 °C for 5 weeks and showed a T_c of 89 K with a ΔT_c of 1.6 K. This crystal had been already characterized previously by various magnetic measurements[12] and had a similar size, namely, $2.9\times1.9\times1$ mm^3.

Temperature dependences of ZFC and FC magnetizations as well as magnetization hysteresis loops were obtained in a commercial Quantum Design 7 T superconducting quantum interference device (SQUID) magnetometer. In most of the experiments, the shielding and pinning currents flowing in the ab plane were of interest; therefore, the field was oriented along the c axis. The measurements were performed with different values of the scan lengths, generally, 3 and 1.5 cm. Both measurements gave essentially the same results, showing the fair homogeneity of the applied magnetic field for almost all the temperature points. The small field inhomogeneity influenced the result for the scan length of 3 cm only in very close vicinity of the irreversibility point. In this case, we varied the scan length step by step and found that the result of the measurement with a 1.5-cm-scan length was not affected by the field inhomogeneity. The usual cooling rate between 50 and 100 K was about 20 K/min (quenching).

In a typical SQUID run, the sample was cooled inside the superconducting magnet in a zero field; then the field was set at 5 K, and the measurement of the sample magnetic moment was performed up to 100 K. The sample was then cooled again with the same cooling rate and the measurement of the FC curves was carried out. Unless mentioned, the FC magnetization was measured during warming [field-cooled warming (FCW)], because field-cooled cooling (FCC) curves cannot be registered in the quenching regime (20 K/min). The magnetization hysteresis loops were taken at several characteristic temperatures.

The sample was attached to a thin high-purity quartz sample holder constructed in such a way to exclude the holder contribution in the SQUID signal. Various methods of sample attachment were employed. We observed that using glue or tape does not affect the result of measurement.

In order to test the dependence of the FC magnetization on the parameters of the cooling process, several additional measurements were performed using slow cooling with a rate of 0.2 K/min. In this case, the magnetization was measured at both cooling (FCC) and warming (FCW). Because the cooling process is also influenced by the sample dimensions, we tested the dependence of the HFPME on the crystal size by cutting the crystal along the ac plane and remeasuring the FC curves thereafter. The HFPME turns out to be size dependent, as reported in the next section.

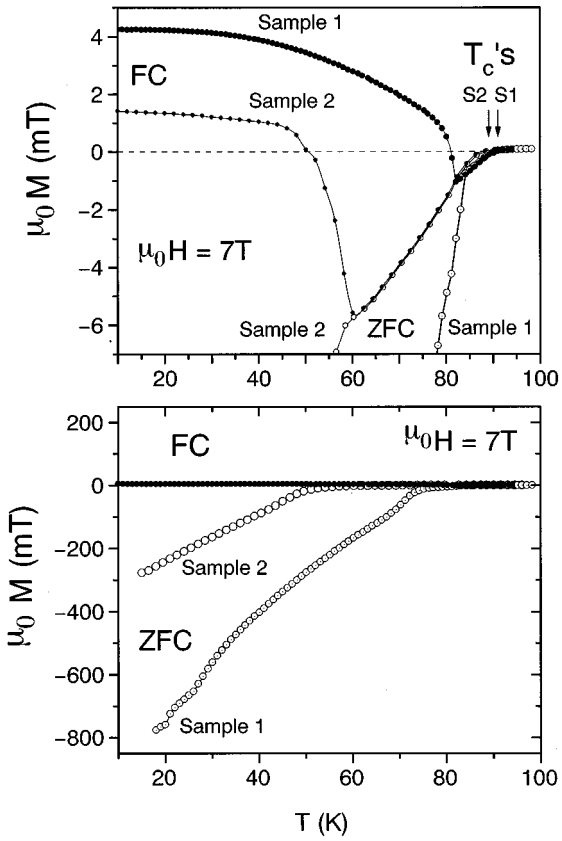

FIG. 1. Zero-field-cooled (ZFC) and field-cooled (FC) magnetizations of the optimally doped single crystal with T_c of 92.3 K (sample 1) and overdoped single crystal with T_c of 89 K (sample 2) at the applied field of 7 T. The top and bottom plots differ by the scale only.

III. RESULTS

Figure 1 shows the typical dependence of the sample magnetizations in the strong fields. Regarding the FC magnetization, its magnitude is comparable in both samples to the value of the reversible magnetization near the irreversibility line $T_{\rm irr}(H)$. For sample 1 at 7 T, the FC magnetization becomes positive below 81 K (Fig. 1). The overdoped sample 2 has a much larger reversible region, but again the paramagnetic moment appears in the broad temperature range below 51 K. In both cases, temperatures of 81 and 51 K lie close to the merging points of the FC and ZFC curves, frequently identified with the irreversibility point. The positive moment is observed when the external field exceeds approximately 4 T. Theoretically, the temperature dependence of the FC magnetization was examined previously; however, no paramagnetic state was derived.[13-16]

In spite of the fact that all the samples studied in this work showed qualitatively similar FC curves, the characteristic temperatures are different. The reversible region was found

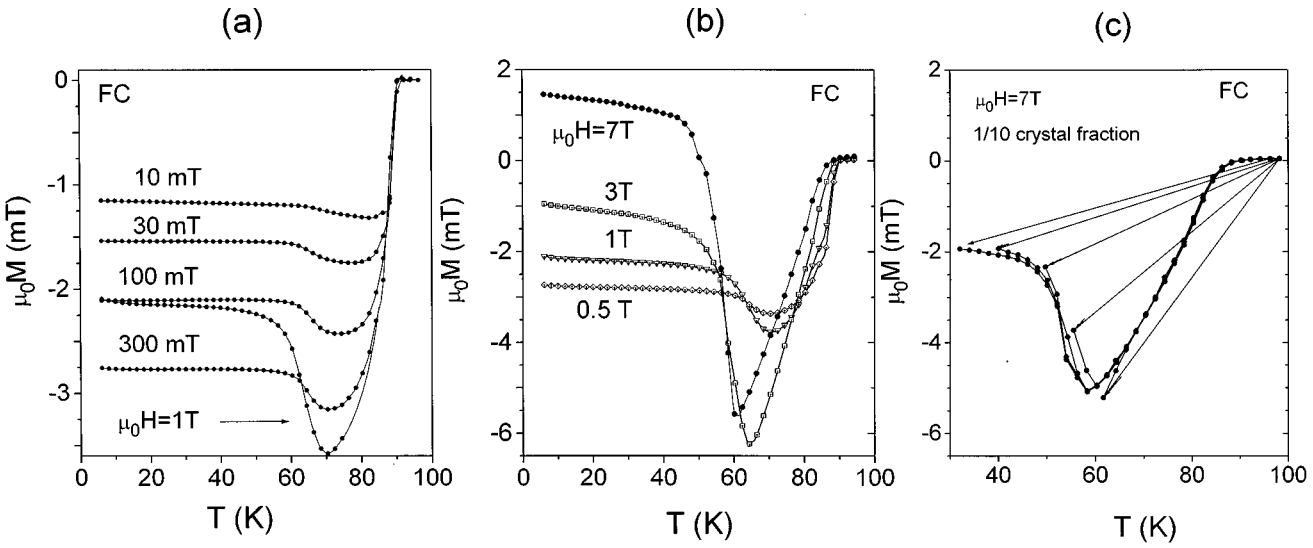

FIG. 2. (a) Field-cooled magnetizations in the overdoped single crystal with T_c of 89 K (sample 2) at the applied field values between 10 mT and 1T. (b) Field-cooled magnetizations in sample 2 at the applied field values between 0.5 and 7 T. (c) Field-cooled magnetizations of the 1/10 fraction of the initial crystal (sample 2), measured from different starting temperatures shown by arrows. The external field is 7 T.

to be larger in the overdoped sample 2. The evolution of the FC magnetization in sample 2 with increasing external field is shown in Fig. 2. From the low-field limit to approximately 300 mT, the magnetization decreases in the whole temperature range below T_c. However, above 500 mT, the FC magnetization continues to decrease only in the region close to T_c [Fig. 2(a)]. Below 60 K, the FC magnetization increases and attains a positive value, which essentially exceeds the magnetization in the normal state [Fig. 2(b)]. This behavior of the magnetization is different from the response of any magnetic impurities. With increasing magnetic field, the dip in the FC magnetization becomes more pronounced and shifts toward lower temperatures. Remarkably, such a dip was observed previously at small fields in the ceramics[18] and single crystals[16] of $YBa_2Cu_3O_{7-\delta}$, as well as in Nb_3Sn.[17] Some of these samples did show the Wohlleben effect at low temperatures, and others showed just a dip, while the susceptibility below the dip did not reach a positive value.[16–19]

In the region of high fields, it appears from Figs. 2(a) and 2(b) that the paramagnetic moments at low temperature and the dip near T_c are closely related. This is because the magnetization at temperatures below the dip increases continuously without any precipitance or singularity around zero magnetization. If we ignore the possibility of flux compression within the framework of the complete Bean state, the FC magnetization goes to zero with increasing external field.[15]

In order to see the dependence of the shape of the FC curve on the sample size and cooling procedure, we employed the following method. Sample 2 was cut into unequal parts along the ac plane and a smaller part of 1/10 initial weight was taken for measurements. As shown in Fig. 2(c), the magnetization below 51 K decreased and became negative. The paramagnetic moment disappeared; however, the characteristic shape of the FC curve remained, showing that the effect of the flux compression is still present.

Using the small part (1/10) of sample 2, we also tested the dependence of the FC curves on the parameters of the cooling process. Because we cooled the sample in the quenching regime with a constant cooling rate, we used the measurement of the FC curve starting from different temperatures [Fig. 2(c)]. In this measurement, only a 2-K undercool was allowed and the cooling rate was constant (20 K/min). The warming rate was kept at 0.5 K/min for all temperature ranges [see arrows in Fig. 2(c)]. The sample was kept for 15 min at the starting point T_s. One can see in Fig. 2(c) that when T_s is below the dip temperature T^*, the FC magnetization increases as T_s approaches to T^*. On the con-

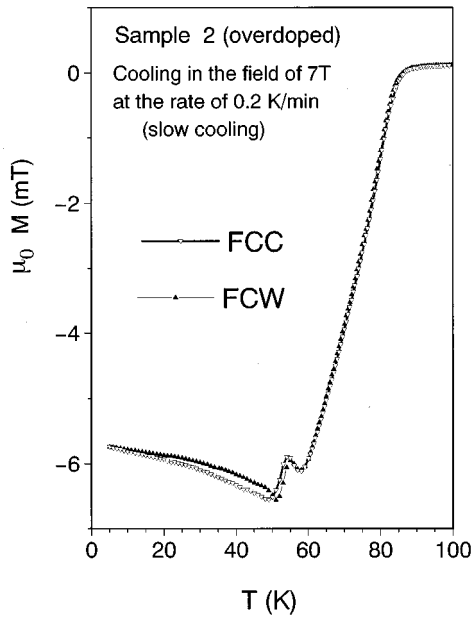

FIG. 3. Field-cooled magnetization of sample 2 measured at cooling (FCC) and at warming (FCW). The cooling rate of 0.2 K/min was 100 times slower than the one in Figs. 1 and 2.

trary, when $T_s > T^*$, the FC magnetization decreases. The result of this measurement suggests that the flux distribution in the sample is affected by the exposure time in the vicinity of T^*. According to the model of flux compression, if the sample is exposed for a certain time at $T_s > T^*$, the flux expulsion outside the sample is more favorable. When $T_s < T^*$, the flux tends to be expelled toward the sample center.

Furthermore, the dependence of the magnetization on the cooling rate was investigated by decreasing the cooling rate down to 0.2 K/min. Under this slow-cooling condition the FC magnetization was measured not only at warming (FCW), but also at cooling (FCC). Both magnetizations measured at cooling (FCC) and at warming (FCW) showed quite similar behavior, without a steep upturn below T^* (Fig. 3). No paramagnetic effect was observed. A small cusp was detected at T^* in both FCC and FCW curves. Most probably the origin of this cusp is related to very small field inhomogeneity. Indeed, near the irreversibility line the pinning of vortices is very weak and the small inhomogeneity of the applied field may produce the removal and backloading of flux during the sample movement between the pickup coils of the SQUID magnetometer. The disappearance of the HFPME with a slow-cooling rate strongly suggests that the paramagnetic moment resulted from rapid sample cooling.

IV. DISCUSSION

A simple way to understand the origin of the dip in the FC curves is to suppose that the time needed for the flux expulsion is insufficient owing to the rapid cooling (20 K/min). Recently, the anomalous dip in the FCW magnetization was explained in terms of a generalized time-dependent critical-state model, using an idea of the nonlinear vortex diffusion.[16] In this model, the dip anomaly deepens when the cooling rate increases.

It is conventionally understood in the intermediate-field range $H_{c1} < H < H_{\rm irr}$ for type-II superconductors that both zero-field-cooled (ZFC) and FC magnetization curves characterize the corresponding Bean *critical* states, which are settled in the cooling process as a result of balance between Meissner diamagnetism and vortex pinning interactions. The details of a suitable critical-state model should account for the sample geometry, and its anisotropic and pinning properties. The magnitude of supercurrents flowing in the critical state largely depends on the magnetic fields, temperature, and sample-specific pinning characteristics. One important parameter which also determines the field and current distributions in the FC critical state is the cooling rate. We showed that by varying this parameter we may change the high-field response of the superconductor from diamagnetic to paramagnetic.

The HFPME observed in this work can be understood as the unusual influence of pinning on the FC magnetization caused by the inhomogeneous cooling and subsequent flux compression in a large crystal, mostly due to its size. In the temperature region close to T_c, in which the vortex motion is strongly enhanced, conventional diamagnetism always appears during the measurement at warming. When this region of rapid vortex motion is crossed quickly on cooling, the time is insufficient for flux diffusion through the thin surface layer, which is rapidly cooled below T_c. Therefore, the flux becomes compressed in the warmer internal region. Since the field range in which the HFPME is observed corresponds to the appearance of the field-induced pinning,[20] some pinning centers may be created at these fields. Subsequently, when the whole crystal becomes uniformly cool, the compressed flux remains trapped on the field-induced pinning centers.

Inhomogeneous flux trapping was also suggested to contribute to the LFPME in Nb foils,[2] in which enhanced pinning may produce a contribution to the hysteresis loops at small fields. The zero-field peak in hysteresis loops may originate not only from pinning, but also from edge barriers.[21] The surface pinning contributes to the magnetic irreversibility at very small fields as well. The quality of the surface was reported to be a key factor which controls the low-field paramagnetic effect in Nb (Ref. 2) and $YBa_2Cu_3O_{7-\delta}$ single crystals (Ref. 22). Kostić *et al.*[2] observed that the paramagnetic signal changes significantly after polishing the surface of Nb foils and suggested that strong surface flux pinning is required for observation of the paramagnetic signal. Zhukov *et al.*[16] proposed a solution for the time-dependent Maxwell equations, in which the dip appears in the FC magnetization and becomes deeper with increasing the cooling rate. In modeling the generalized time-dependent critical state, the authors[16] neglected the influence of the geometrical[21] and Bean-Livingston[23] surface barriers on the nonlinear flux diffusion. It would then be possible to connect the LFPME in Nb with surface magnetization. Indeed, edge barriers and the rapid cooling would affect the flux distribution in a similar way, yielding a deeper FCW anomaly near T^*. However, we may preclude that if the reason for the PME were the edge barriers only, the PME might disappear if the cooling rate is sufficiently reduced.[24] Contrary to such a situation arising eventually when the LFPME is influenced by surface effects, it was shown for the Wohlleben effect in granular superconductors that paramagnetism is reduced at rapid enough cooling (faster than 12 K/min), but does not change if the cooling rate is slower than 12 K/min.[25]

The experiments performed recently by Magnusson *et al.*[10,11] in the granular superconductors show that positive magnetization increases with time. The positive logarithmical relaxation agrees with the theoretical estimate for the system of polarizable superconducting current loops.[10,26] These experiments strongly suggest the nontrivial origin of the LFPME in granular superconductors.[10,11] A similar mechanism could also be relevant for the HFPME because of the granular behavior which the single crystals show in a strong field,[20,27,28] in contrast to the fact that high-quality single crystals are fully coupled in a low field. Competing on equal terms with the flux compression model, the orbital glass scenario could be implemented as well in the HFPME.[29] The intragrain granularity which is induced in a strong field and associated with the fishtail effect[20,28] could be at the origin of the orbital-glass behavior in the latter case.

Regarding the HFPME, we will comment on the behavior of the magnetic hysteresis loops around T^*. We will then discuss the HFPME from the viewpoint of the peak effect in high-field magnetization curve. As shown in Fig. 4, in both samples, the second peak arises in magnetization loops below T^*. It was previously found that the temperature depen-

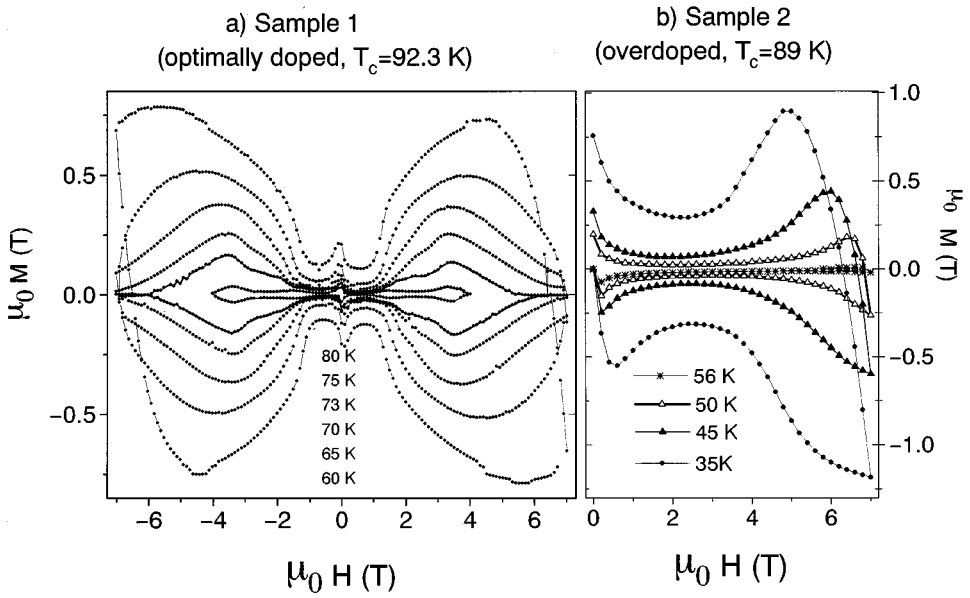

FIG. 4. Magnetization hysteresis loops in samples 1 and 2.

dences of both the irreversibility field and the field of the second peak (fishtail) are steeper in the overdoped samples than in the optimally doped samples. In other words, the second peak in the magnetization loops shifts towards higher fields in the overdoped sample at low enough temperatures.[12,27] Indeed, one sees in sample 1 that the fishtail maximum within 20 K just below T^* (81 K) is positioned in the accessible range of fields, while in sample 2, the second maximum is centered beyond the upper limit of our SQUID (7 T), but the tail of the peak clearly appears in our field range. The curves of critical current vs the applied field show minima at 0.8 and 2.7 T in samples 1 and 2, respectively. With increasing field these minima are followed by a sharp increase of the critical current. The peak field shifts dramatically by varying the oxygen content. Thus, field-induced pinning is strongly affected by variation of the doping level. Primarily, it can be understood as an effect of change in anisotropy λ_c/λ_{ab} and ξ_c/ξ_{ab}. An additional reason for the shift of the peak field and irreversibility line may arise from modifying the type of pinning centers, which could be dependent on the oxygenation process.

In the series of samples, we measured the dip temperature T^* for various oxygen contents. From a comparison of the values of T^* with the temperature dependence of the second peak, we may associate the HFPME with the enhancement of the pinning efficiency in the region of the second peak. Indeed, by comparing Figs. 1 and 4 one can find a correspondence between the temperature range for the appearance of the pronounced fishtail and HFPME.

The close relationship between the fishtail effect and the HFPME was also established by measurements of the hysteresis loops and FC magnetizations on the same sample, but loaded with different oxygen contents.[27] Here again, the critical current in the field range of the second peak begins to increase rapidly just below the dip temperature T^*, which shifts in accordance with the value of the oxygen deficiency δ. The fishtail effect in $YBa_2Cu_3O_{7-\delta}$ is known to be linked with the oxygen deficiency.[20,28] As a common phenomenon for the large family of the conventional and high-T_c superconductors,[31] this effect weakens with decreasing disorder (pointlike, twinning). In our $YBa_2Cu_3O_{7-\delta}$ crystals, both the fishtail and HFPME are strongly affected by the oxygen content $7-\delta$.[12,27] This may signify that the field-induced pinning centers are related to the oxygen deficiencies. Although we cannot specify the exact manner of interference between the oxygen vacancy distributions and the magnetic field to produce efficient pins, we may suppose that these pins could also compress the flux lines. In the regime of strong pinning,[32] all the pinning centers can be occupied by vortices, but some extra vortices may take advantage of being inside the strong pinning center.

Recently, a similar scheme of flux compression around the scratch on the surface was proposed by Flippen *et al.*[33] in the study of thin (below 0.1 mm) $YBa_2Cu_3O_{7-\delta}$ single crystals. The scratches are strong surface pinning centers and they tend to bend and shift the flux lines to confine a number of vortices within the pinning center. Such a multiple-center flux compression induces the local depletion of the density of vortices around the scratch. In this depleted area, the circular current is flowing around the strong pinning center and we may associate a paramagnetic moment with this circular current. Because the effects of the surface manifest themselves at small fields, the surface pinning and the paramagnetic moments associated with the circular currents around the surface imperfections could be at the origin of the low-field PME. This mechanism is the most plausible one for the Nb foil;[2,3] however, it might not be unique.

It is noteworthy that the mechanism of flux compression suggested by Koshelev and Larkin[1] in the range of small fields is applicable only to the special platelike geometries of the sample oriented perpendicularly to the field. If the entire flux is trapped in the cylindrical samples extended along the field direction, the moments of two coaxial current rings, pinning current, and shielding current are canceled and no net paramagnetic moment is expected.[1] However, we observed the paramagnetic moment for the thick bulky crystals in the range of high fields. This allows us to argue that a similar configuration of the flux-free surface layer[1] is implausible and the Koshelev-Larkin mechanism may not be directly applicable to the examinaion of the HFPME.

On the other hand, one may also suggest a scenario in which the orbital glass could be generated at fast cooling in a strong magnetic field. In this FC quenching process, the superconductor first enters the vortex liquid state above the irreversibility line. Due to presence of the field-induced pinning centers, the order parameter may exhibit a long-scale inhomogeneity and there arise the nucleons of the vortex bundles, which are decoupled from each other by the vortex liquid. There occurs a pinning current around each bundle and a phase coherence exists within the bundle. Each nucleon possesses its own phase and a Josephson coupling exists between the bundles. In the case when the superconducting order parameter has unconventional symmetry, each nucleon may possess a different orientation of the order parameter. With decreasing temperature, when the superconductor enters the irreversible region of the *H-T* diagram, the bundles become strongly coupled and the disorientation of the order parameter between them may produce the current topological defects, like π rings.[7–9] The orbital moments associated with the latter defects constitute an orbital glass and can be polarized. In this scenario, the fact that the HFPME strongly depends on the cooling rate indicates that the topological defect density increases with increasing cooling rate; that is, the different phases of the order parameter in different nucleons can be quenched at fast cooling. On the contrary, at slow cooling the order parameter at different field-induced ''grains'' has sufficient time to relax to the same orientation and spontaneous circular currents do not appear.

The most interesting issue of the present study is why the paramagnetic effect in the superconductors arises only at very small or very high fields. This problem is closely related to the question of why the two peaks exist in the magnetization hysteresis loops. Since the compression of the magnetic flux may occur both at the surface and in the bulk, the two peaks in $M(H)$ hysteresis loops indicate the field ranges wherein the compressed flux can be trapped effectively. On the other hand, these field regions correspond to the existence of weak links in the naturally granular materials or in the materials with field-induced granular behavior. The origin of the high-field paramagnetic effect might be better clarified as soon as the nature of the puzzling fishtail effect is established.

V. CONCLUSION

We have observed the paramagnetic moment at a strong magnetic field ($H_{c1}<H<H_{c2}$) in field-cooled $YBa_2Cu_3O_{7-\delta}$ single crystals after rapid cooling. This effect is sensitive to the cooling rate and sample size, which suggest that inhomogeneous cooling of the large crystals causes this effect. It is shown that the temperature at which the HFPME sets in coincides with the temperature at which the $M(H)$ curves start to exhibit a very pronounced fishtail effect. Therefore, the HFPME may be linked with the second peak, which is typically observed in the magnetization hysteresis below $T_{irr}(H)$. In other words, we associated the HFPME with the puzzling ''fishtail''-like shape of the hysteresis semiloops. The effect may appear in the course of autocompression of the flux on the field-induced pinning centers, or it may also be associated with current path topological defects originating from the oxygen deficiencies.[8,9] On the other hand, such defects may also play the main role in the ''fishtail'' effect.

ACKNOWLEDGMENTS

This work has been supported by NEDO for the Research and Development of Industrial Science and Technology Frontier Program.

*Permanent address: Loughborough University, Loughborough, Leicestershire, LE11 3TU, United Kingdom.

[1] A.E. Koshelev and A.I. Larkin, Phys. Rev. B **52**, 13 559 (1995).
[2] P. Kostić, B. Veal, A.P. Paulikas, U. Welp, V.R. Todt, C. Gu, U. Geiser, J.M. Williams, K.D. Carlson, and R.A. Klemm, Phys. Rev. B **53**, 791 (1996).
[3] M.S.M. Minhaj, D.J. Thompson, L.E. Wenger, and J.T. Chen, Physica C **235-240**, 2519 (1994).
[4] P. Svedlindh, K. Niskanen, P. Norling, P. Nordblad, L. Lundgren, B. Lönnberg, and T. Lundström, Physica C **162-164**, 1365 (1989).
[5] W. Braunisch, N. Knauf, V. Kataev, S. Neuhausen, A. Grütz, A. Kock, B. Roden, D. Khomskii, and D. Wohlleben, Phys. Rev. Lett. **68**, 1908 (1992).
[6] W. Braunisch, N. Knauf, G. Bauer, A. Kock, A. Becker, B. Freitag, A. Grütz, V. Kataev, S. Neuhausen, B. Roden, D. Khomskii, and D. Wohlleben, Phys. Rev. B **48**, 4030 (1993).
[7] M. Sigrist and T.M. Rice, Rev. Mod. Phys. **67**, 503 (1995).
[8] F.V. Kusmartsev, Phys. Rev. Lett. **69**, 2268 (1992).
[9] F.V. Kusmartsev, Phys. Lett. A **169**, 108 (1992).
[10] J. Magnusson, J.-O. Andersson, M. Björnander, P. Nordblad, and P. Svedlindh, Phys. Rev. B **51**, 12 776 (1995).
[11] J. Magnusson, M. Björnander, L. Pust, P. Svedlindh, and P. Nordblad, Phys. Rev. B **52**, 7675 (1995).
[12] A.I. Rykov, W.J. Jang, H. Unoki, and S. Tajima, in *Advances in Superconductivity VIII*, edited by H. Hayakawa and Y. Enomoto (Springer-Verlag, Tokyo, 1996).
[13] T. Matsushita, E.S. Okabe, T. Matsuno, M. Murakami, and K. Kitazawa, Physica C **170**, 375 (1995).
[14] J.R. Clem and Z. Hao, Phys. Rev. B **48**, 13 774 (1993).
[15] Y. Tomioka, M. Naito, K. Kishio, and K. Kitazawa, Physica C **223**, 347 (1994).
[16] A.A. Zhukov, A.V. Volkozub, and P.A.G. de Groot, Phys. Rev. B **52**, 13 013 (1995).
[17] O.B. Hyun, Phys. Rev. B **48**, 1244 (1993).
[18] T. Ishida, R.B. Goldfarb, S. Okayasu, and Y. Kazumata, Physica C **185-189**, 2515 (1991).
[19] J. Schaf, P. Rodrigues, Jr., L. Ghivelder, P. Pureur, and S. Reich, Physica C **247**, 376 (1995).
[20] M. Daeumling, J.M. Seuntjens, and D.C. Larbalestier, Nature **346**, 332 (1990).
[21] E. Zeldov, A.I. Larkin, V.B. Geshkenbein, M. Konczykowski, D. Majer, B. Khaykovich, V.M. Vinokur, and H. Shtrikman, Phys. Rev. Lett. **73**, 1428 (1994).
[22] R. Lucht, H.v. Löhneysen, H. Claus, M. Kläser, and G. Müller-Vogt, Phys. Rev. B **52**, 9724 (1995).
[23] M. Konczykowsky, L.I. Burlachkov, Y. Yeshurun, and F. Holtzberg, Phys. Rev. B **43**, 13 707 (1991).
[24] The Bean-Livingston and geometrical or edge barriers indeed may be responsible for the PME if the flux were trapped. If we cool slowly enough so that the trapped vortices could escape

through these barriers, the PME may also disappear.

[25] Yu. He, C.M. Muirhead, and W.F. Vinen, Phys. Rev. B **53**, 12 441 (1996).

[26] F.V. Kusmartsev, J. Supercond. **7**, 617 (1994).

[27] A.I. Rykov and S. Tajima (unpublished).

[28] J.L. Vargas and D.C. Larbalestier, Appl. Phys. Lett. **60**, 1741 (1992).

[29] At high fields (4–7 T), we performed the relaxation measurements (Ref. 30), in which the FC magnetization was recorded for several hours at a fixed temperature, and observed the slow increase of the positive FC magnetization with time, which accordingly suggests the possibility of the nontrivial origin of the HFPME.

[30] A.I. Rykov, S. Tajima, and F.V. Kusmartsev, in *Advances in Superconductivity IX*, edited by S. Nakajima and M. Murakami (Springer-Verlag, Tokyo, in press).

[31] V. Hardy, A. Wahl, A. Ruyter, A. Maignan, C. Martin, L. Coudrier, J. Provost, and Ch. Simon, Physica C **232**, 347 (1994).

[32] A.I. Larkin, M.C. Marchetti, and V.M. Vinokur, Phys. Rev. Lett. **75**, 2992 (1995).

[33] R.B. Flippen, T.R. Askew, J.A. Fendrich, and C.J. van der Beek, Phys. Rev. **52**, R9883 (1995).